JOURNAL OF MATERIALS SCIENCE **20** (1985) 3590–3596

The voltage–current characteristics of thin MIM sandwiches with SiO_x/Bi_2O_3 as the insulator

K. I. ARSHAK, A. GLOT*, C. A. HOGARTH
Department of Physics, Brunel University, Uxbridge, Middlesex, UK

Regions of current-controlled and voltage-controlled negative resistance (CCNR and VCNR) have been observed in thin films of Bi_2O_3/SiO_x with aluminium electrodes. ESCA measurements revealed the formation of metallic bismuth impurities in the dielectric, associated with a small activation energy for conductance, prior to any electroforming process. With copper electrodes only VCNR was observed. These thin films have been found to possess relatively high concentrations of dangling bonds.

1. Introduction

A number of materials in the form of thin insulating films sandwiched between metal electrodes (MIM structures) have been found to exhibit negative resistance effects after undergoing a forming process [1]. There are two types of negative resistance which are distinguished by the general shape of their current–voltage characteristics. These are the N-type voltage-controlled negative resistance (VCNR) and the S-type current-controlled negative resistance (CCNR) [2]. In most cases any particular sample demonstrates only one type of negative resistance after a suitable forming process. Materials that usually show VCNR on their *V–I* characteristics are oxides, halides, and some organic and polymeric substances, while chalcogenide and certain oxide glasses normally show S-type negative resistance.

The co-evaporation technique described by Hogarth and Wright [3] was used to prepare a new insulator material and it was possible to observe the two forms of negative resistance on the same glass substrate. For this purpose a composite film made of Bi_2O_3 and SiO_x was used. An S-type negative resistance was observed on the bismuth oxide-based structures after switching to the low-resistance state [4], and N-type characteristics were found for silicon oxide thin films after forming in accordance with well-known results [1, 5]. In this paper the results of an experimental study of the SiO_x/Bi_2O_3 thin film system are presented.

2. Experimental work

The samples for the electrical measurements were prepared on cleaned 1 in × 3 in (2.54 cm × 7.62 cm) 7059 Corning glass substrates by vacuum deposition of successive layers of metal–insulator–metal under pressures of about 2×10^{-6} torr in a Balzers BA510 coating unit using the technique described by Hogarth and Wright [3], with a substrate temperature of ~ 100° C. Two types of configuration were used for fabrication of the devices, as shown in Fig. 1. Tungsten and tantalum boats were used for the evaporation of the Bi_2O_3 and the SiO, respectively. The thickness of each of the films was monitored using a quartz crystal monitor. The electrode thickness was kept between 70 and 90 nm. The molecular percentage of Bi_2O_3 in the same oxide layer was kept at 10%. The active area of the top electrode of the specimen reported in Fig. 1a was 0.071 cm^2 and that of the specimen of Fig. 1b was 0.15 cm^2. The electrical measurements were carried out in a

---

*Permanent address: Dneipropetrovsk State University, Dneipropetrovsk, USSR.

0022–2461/85 $0.300 + .12

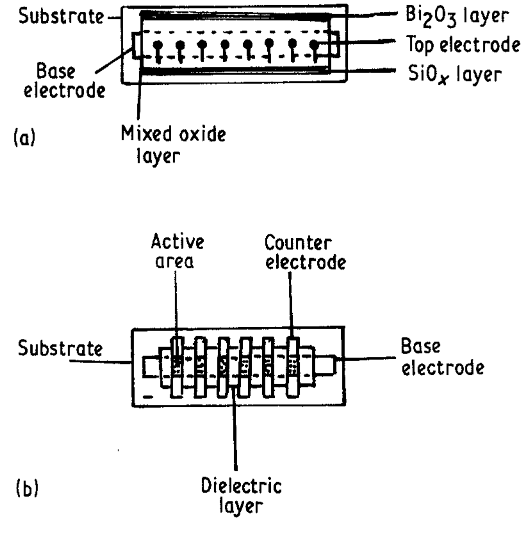

Figure 1 Two types of sample arrrangement used for the study of voltage–current characteristics. Active area (a) 0.071 cm^2, (b) 0.15 cm^{-2}.

subsidiary vacuum system capable of producing a vacuum of 10^{-6} torr. Temperature measurements were made by attaching a copper–constantan thermocouple to the substrate by means of silver paste. Lowering the device temperature was achieved by pouring liquid nitrogen into a cryostat which was firmly attached to the base of the sample by means of pressure contacts. The d.c. voltage–current characteristics were measured using conventional methods. For the measurements of ESR, fused silica glass substrates of length 3 cm and width 1 cm and which had been fused on to special mounting rods to fit the resonant cavity of the Varian E-3 EPR spectrometer, were held at a temperature of 100° C.

The electron spectroscopy for chemical analysis (ESCA) technique has been used to provide information about contaminant species and the compositions of each oxide constituent. The ESCA spectra were recorded on a Kratos ES 350 spectrometer using Al*Kα* X-rays as the excitation source. The working pressure in the chamber was better than 10^{-7} torr. In order to calibrate the binding energy scale of the spectra, the C(1s) level arising from oil contamination was taken as 284.6 eV.

3. Results

3.1. Spectroscopic analysis

Fig. 2 shows a typical ESCA spectrum of the mixed oxides of the complex Bi_2O_3/SiO_x thin film. It is evident from the figure that of all the specified electronic levels of bismuth and silicon, the 4f levels of bismuth give the strongest ESCA signals. The 2p level for silicon as well as a partial survey scan of energies in the range of O 1s up to C 1s are shown in the same figure.

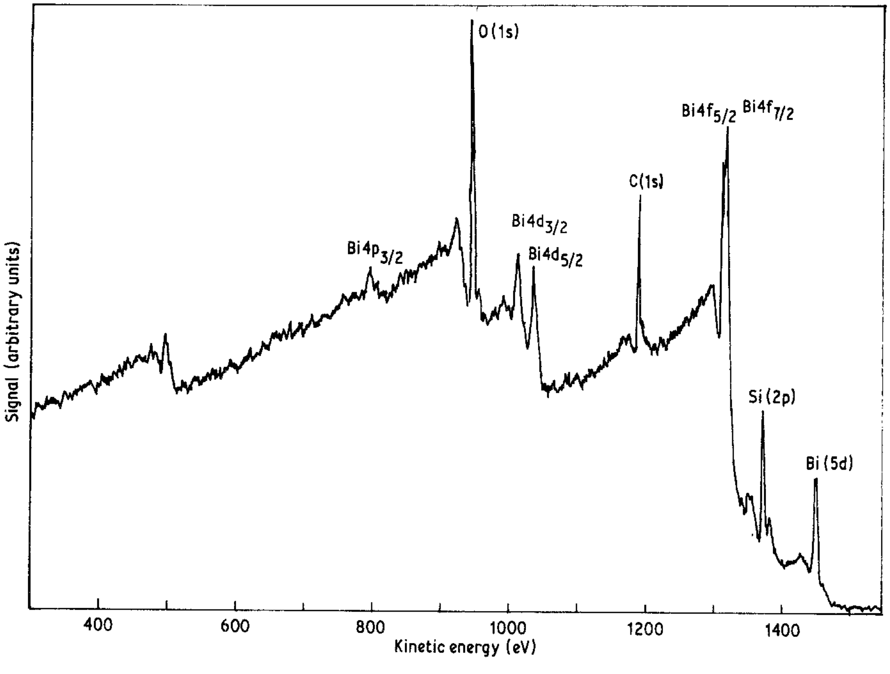

Figure 2 Partial survey scan for a thin film of the mixed oxide complex SiO/Bi_2O_3 in thin film form.

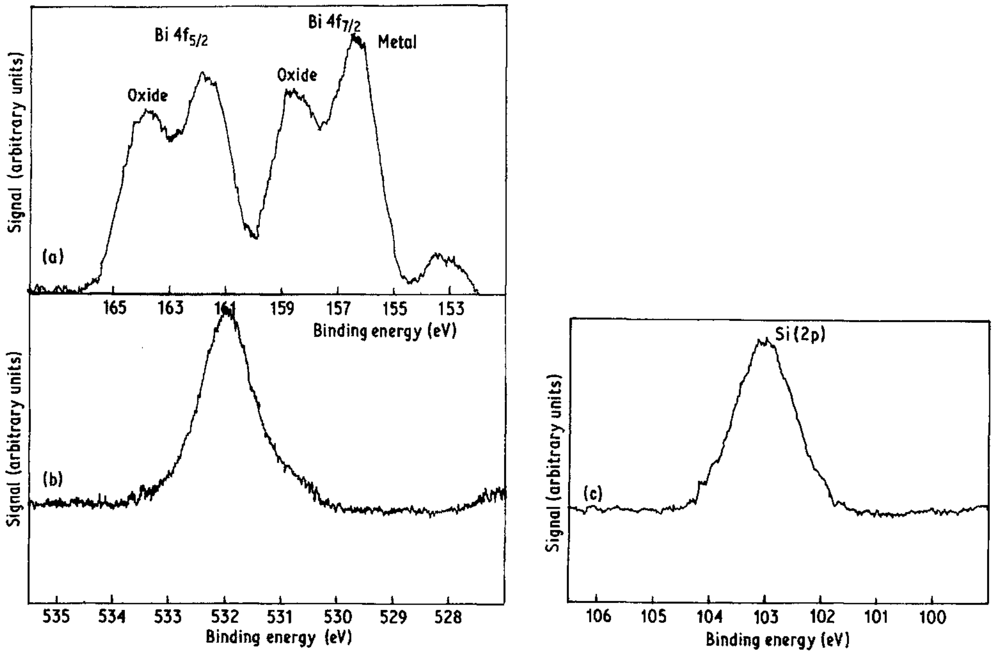

Figure 3 ESCA spectra (a) Bi $4f_{5/2}$–Bi $4f_{7/2}$ spectra (b) O(1s) spectrum. (c) Si(2p) spectrum.

Careful consideration of this spectrum shows the duplex nature of bismuth 4f levels in contrast to the same level in silicon. Fig. 3a shows the narrow scan of the ESCA spectrum of bismuth and illustrates the chemical shift in the film matrix. The 4f level in bismuth is split into a natural doublet ($4f_{5/2}$ and $4f_{7/2}$) due to spin-orbit coupling. Two peaks are found in each of these levels, with the higher peaks being due to the metallic bismuth of the film and the lower peaks to the bismuth oxide. For these reasons the complex of Bi_2O_3/SiO_x forms a thin film of fairly high conductivity. Fig. 3b shows the O 1s spectral scan for the sample and Fig. 3c shows the silicon Si 2p spectra from which the binding energy is found to be 102.8 eV which is in good agreement with the standard reported value for SiO_2 of 103.4 eV and indicates that the evaporated element in the matrix of the film is SiO_2 rather than SiO. The derived values of the binding energies are given in Table I.

Two films of mixed SiO_x and Bi_2O_3 of thickness of the order of 300 nm and fixed compositions (10% Bi_2O_3/90% SiO) but having different values of R/p (R being the rate of deposition and p the partial pressure inside the chamber during the evaporation) were made. Fig. 4 shows the ESR spectra for two samples of thin SiO_x/Bi_2O_3 films of thickness 300 nm measured at $g = 2.00$ and at room temperature, for different values of R/p but having the same composition nominally 90% SiO/10% Bi_2O_3. The general form of the signal is the same as that of SiO except that the strength of the signal decreases as R/p is decreased. The second integral of these curves is directly proportional to the spin density and the absolute values were calculated by comparing with the known spin concentration of aqueous copper sulphate solution. It was found that the film of high R/p ($0.54 \times 10^6\,nm\,sec^{-1}\,torr^{-1}$) had a spin density of $6.5 \times 10^{18}\,cm^{-3}$, whereas for the film for

TABLE I Derived binding energies of bismuth, oxygen, silicon and carbon in a co-evaporated thin complex film of SiO_x/Bi_2O_3

	Bi $4f_{5/2}$		Bi $4f_{7/2}$		O 1s	Si 2p	C 1s
	Oxide	Metal	Oxide	Metal			
Binding energy (eV)	164.5	162.5	159.5	157.5	532.4	102.8	1480

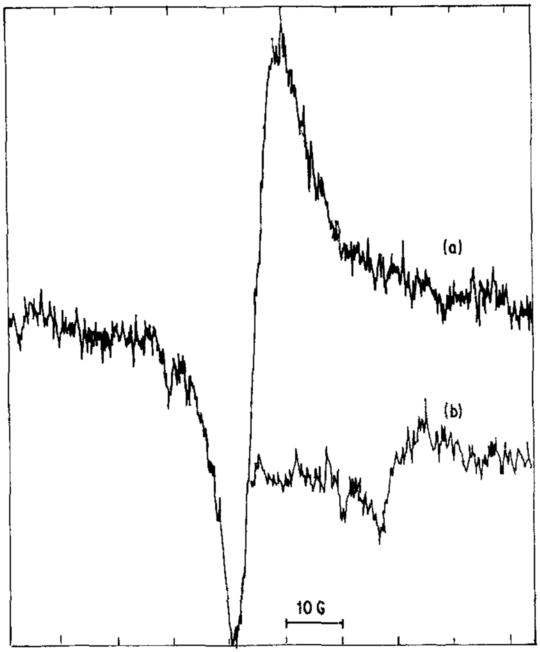

Figure 4 ESR spectra of SiO/Bi_2O_3 mixed films 200 nm thick of composition 90 mol % SiO/10 mol % Bi_2O_3. (a) High R/p, (b) lower R/p.

which R/p was $0.4 \times 10^5\,nm^{-1}\,torr^{-1}$ the spin density was $1.0 \times 10^{18}\,cm^{-3}$.

3.2. Electroforming and related phenomena

In order to understand the conduction prior to electroforming, samples of thickness 200 nm and composition 90 mol % SiO_x/10 mol % Bi_2O_3 and with aluminium top and base electrodes were used for the study of voltage–current characteristics. Measurements below and above room temperature were also taken. The voltage–current characteristics (VCC) of a thin film sandwich are presented in Fig. 5 (aluminium electrodes) and Fig. 9 (copper electrodes). All samples demonstrated non-ohmic behaviour. The initial characteristic (curve 1 in Fig. 5) was non-linear and reproducible unless a critical value of current ($\sim 10^{-4}$ A) was reached. Above this value, the current flowing through the device became unstable and irreversible changes of characteristic were observed (forming process). For the device with aluminium electrodes we distinguish two stages of forming process. After the first stage of the forming process CCNR was observed (curve 2 in Fig. 5). This characteristic was recorded several times. However, a subsequent increase of voltage produced no CCNR and the current continued to increase with voltage until the second stage of forming was reached (curve 3 in Fig. 5). At this stage the characteristic transferred as shown in Fig. 5 to curve 4 which is typical of a normal characteristic for a formed MIM device showing an augmented conductivity and a negative resistance region.

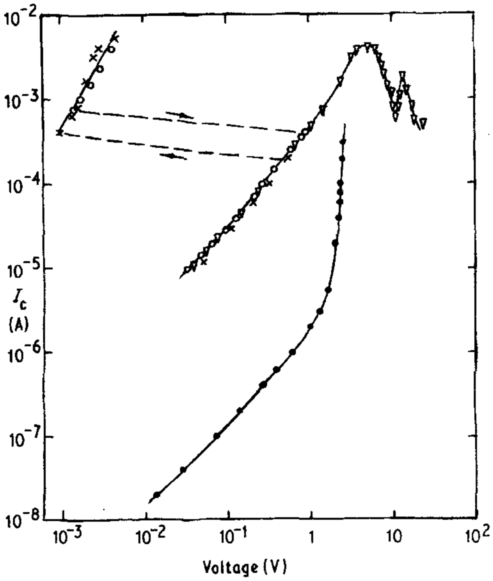

Figure 5 Voltage–current characteristics for an MIM structure in which the metal, M is aluminium and the insulator, I is 90 mol % SiO/10 mol % Bi_2O_3. ● 1, × 2, ○ 3, ▽ 4.

These apparently anomalous results may be explained as follows. It is known that electroforming of MIM oxide structures can take a significant time, e.g. of the order 40 min at a minimum forming voltage when aluminium electrodes are used, so that before the initial forming is complete, other phenomena may arise. In the present work the CCNR is believed to arise from a punching through of the space-charge region in the insulator to the further electrode giving S-type switching. Once, however, the normal forming process is complete, i.e. the polyfilaments have been established across the insulator, the normal N-type (VCNR) curve is expected and indeed is observed. After this the CCNR is no longer observed on the sample tested. As will be reported later, CCNR is not observed when the electrode material is one, such as copper, which can diffuse much more rapidly into the oxide so that electroforming is completed in a few seconds. In these circumstances

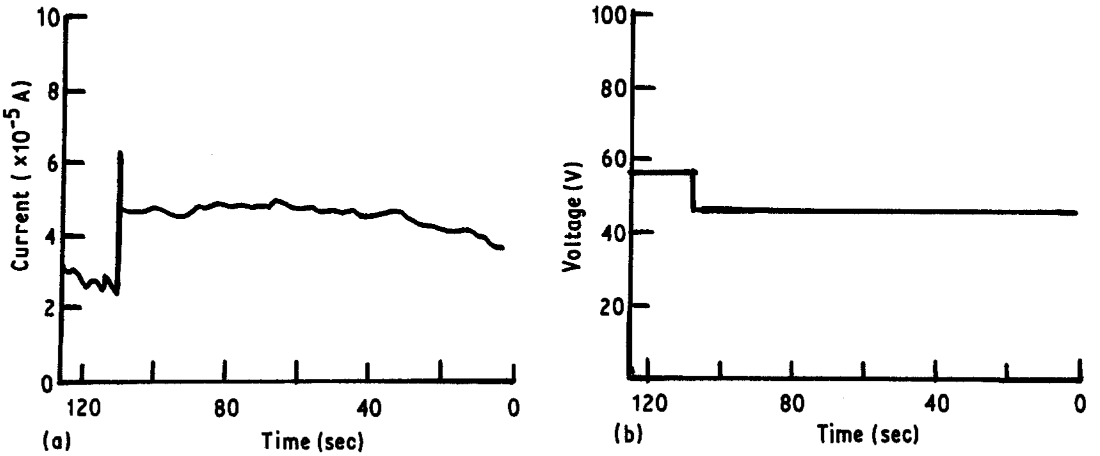

Figure 6 Time dependence of (a) current and (b) voltage taken directly from a chart recorder for a thin film sample with aluminium electrodes.

VCNR is quickly established. Fig. 6 shows in a graphic way how the sample operates in this negative resistance region and traces of the time dependence of voltage and current, recorded simultaneously, are presented. It is obvious that the increase of voltage produces a decrease of current.

After the treatment described above, the samples were examined under the scanning electron microscope SEM in order to study the structure of the dielectric film. An argon ion bombardment of the device was carried out to etch away the counter-electrodes of a device left in the conductive state. It was observed that there is no obvious termination of filaments at the surface, but damage to the aluminium electrodes of the sample was indicated at the top electrode after the forming process. The nature of this phenomenon is not fully understood but is probably related to the damage caused to aluminium overlays in integrated circuits as a result of the current flowing through them [6]. Attempts were made to find conductive channels or filaments by using argon beam etching and the SEM together with microprobe analysis techniques. Preliminary results show an increase of aluminium and a decrease of bismuth in damaged areas revealed by Fig. 7 which shows an SEM picture of the affected area and gives an idea of the local displacement of the aluminium electrode, so that aluminium may be distributed locally and may screen the underneath dielectric

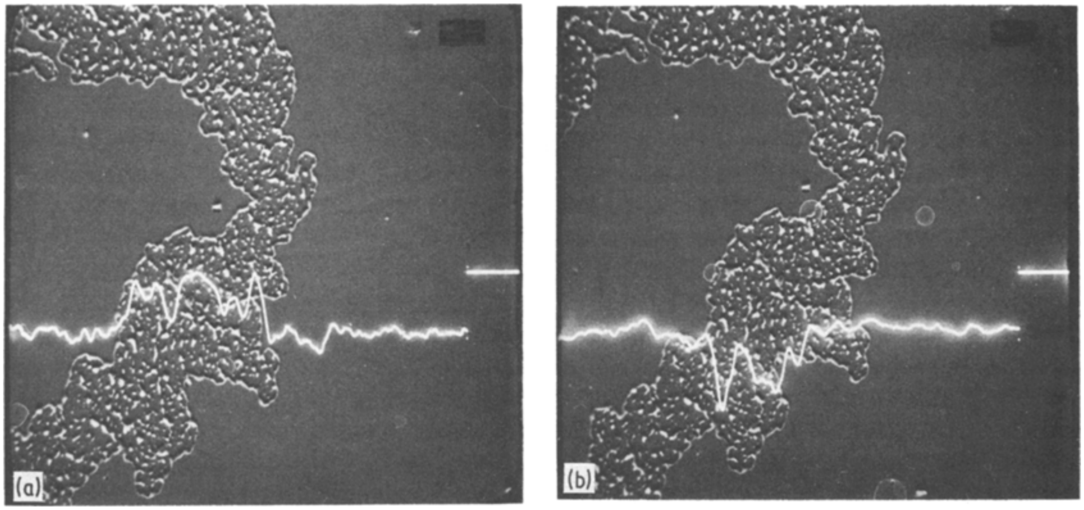

Figure 7 Electron micrographs showing the damage to the active area caused by the application of a voltage and showing the X-ray miocroprobe scan lines for (a) aluminium and (b) bismuth.

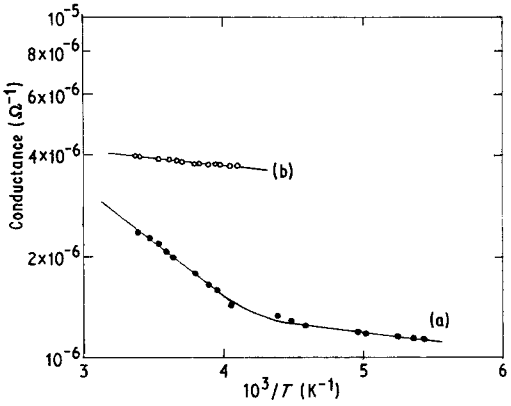

Figure 8 Conductance as a function of inverse temperature at 0.4 V applied (a) before electroforming, (b) after electroforming for a mixed SiO_x/Bi_2O_3.

which contains bismuth, thereby reducing the bismuth signal. The high Joule heating of local regions of the sample leading to the redistribution of aluminium may well be responsible for the relatively slow increase of current at constant voltage as shown in Fig. 8. The increase of voltage accelerates this process. However, it takes a relatively long time to reach the steady state. The ion migration during filament formation may partly contribute to this slow process. As far as metallic bismuth was found in our samples, as revealed in Fig. 2, and knowing that aluminium does not diffuse rapidly inside the dielectric (concentration of aluminium did not decrease, as seen in Fig. 7), bismuth ions may be mobile inside the sample. The metallic fraction of bismuth is repsonsible for the low activation energy for conductance in the initial state (i.e. before forming) which is shown by Fig. 8a. After forming, the activation energy becomes even less than that before forming as shown in Fig. 8b and this is due to the formation of bismuth-rich conductive paths inside the Si–Bi–O dielectric.

3.3. Voltage–pressure memory effect

A sample of thickness 300 nm having the configuration of Fig. 1b was electroformed and its *V–I* characteristic shown in Fig. 9 has a pronounced and reproducible VCNR region under good vacuum conditions. Upon increasing the ambient pressure to atmospheric, the same characteristic may be traced up to 4 V; beyond this a reduction in the conductivity occurred, exhibiting VCNR followed by some fluctuation in the current level beyond 35 V. On decreasing the voltage gradually to zero, the device demonstrated the pressure–memory effect which was maintained in further runs. This effect could be attributed to the voltage-stimulated adsorption of oxygen which immobilized the conducting electrons as described earlier [7]. The shift in the VCNR region and the associated current fluctuations may be explained by the same effect decribed above associated with the pressure-induced changes in the distribution of the conducting filaments [8]. It may be noted that free copper in Cu_2O films may lead to switching phenomena [9].

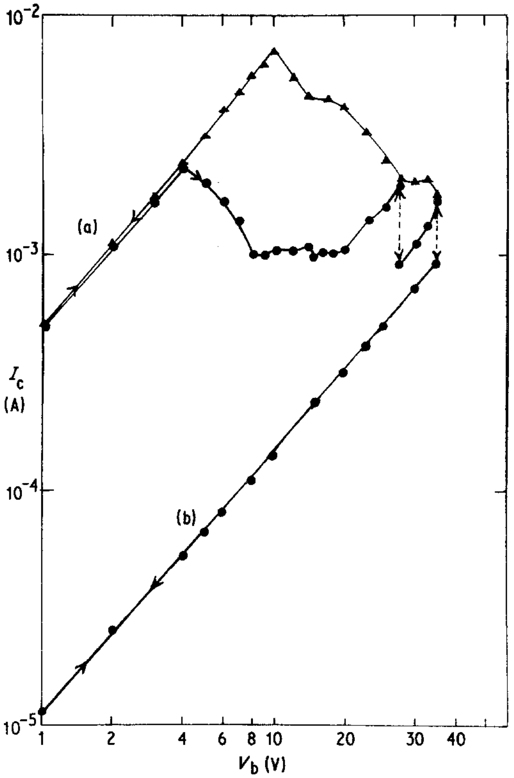

Figure 9 Voltage–current characteristics for a formed film of $Cu–SiO/Bi_2O_3–Cu$ (a) at 10^{-6} torr, (b) at atmospheric pressure.

4. Discussion and conclusions

As we observed from the ESCA analysis there is some metallic bismuth inside the dielectric which may well form impurity bands which could then be responsible for the low activation energy calculated from the conduction data. This metallic bismuth is relatively weakly connected to the chemical and structural network of the dielectric oxide, and this could lead to the possibility of the bismuth atoms or ions moving under the influence of an electric field and Joule heating during the forming process. The establishment of VCNR in all samples and the occurrence of CCNR in samples carrying aluminium electrodes, which is observed *before* the VCNR is established have been discussed in Section 3.

The film of SiO_x/Bi_2O_3 deposited at a high value of the R/p parameter and having a high spin density ($\sim 6.5 \times 10^{18} cm^{-3}$) seems to exhibit two kinds of conduction mechanism, namely hopping at low field and low temperature and free-band conduction at higher temperatures. The activation energies for the two mechanisms are 0.01 and 0.06 eV, respectively. Al-Ismail and Hogarth [10] have demonstrated similar behaviour in 100% SiO_x films, the only difference being the sharp transition from hopping to free-band conduction reported earlier [11] for samples having a higher spin density of almost $10^{20} cm^{-3}$.

The strong dependence of high field d.c. conductivity on R/p for SiO has been known for some time [12, 13]. The concept of a compensated disordered solid may be considered for the explanation of the variation of the number of unpaired electrons (spin density) with the parameter R/p, as follows. The donor levels will be assumed to be the centres responsible for conduction. Trap levels produced by defects will exist throughout the band gap of the solid material at a density varying between 1×10^{18} to $6.5 \times 10^{18} cm^{-3}$ and act as compensators to donor states. In films with a high value of spin density ($6.5 \times 10^{18} cm^{-3}$), which have high values of R/p, the donor density must be larger than the trap density, since the compensation is incomplete and there are some electrons left in the donor centres, showing uncompensated properties. For lower donor densities of $\sim 10^{18} cm^{-3}$, partial compensation takes place, which then reduces the number of occupied centres and hence, the conductivity. One can explain the reduction in the value of the spin density from 6.5×10^{18} to $1 \times 10^{18} cm^{-3}$ when the value of R/p has been reduced from 0.54×10^6 nm sec^{-1} torr^{-1} to 0.4×10^5 nm sec^{-1} torr^{-1} as due to the reactive evaporation which can reduce the concentration of centres by oxidation to $\sim 1 \times 10^{18} cm^{-3}$ which is probably the concentration of traps in the forbidden band gap of the mixed Bi_2O_3/SiO_x films.

References

1. G. DEARNALEY, D. V. MORGAN and A. M. STONEHAM, *J. Non-Cryst. Solids* **4** (1970) 595.
2. F. ARGALL, *Electron. Lett.* **2** (1966) 282.
3. C. A. HOGARTH and L. A. WRIGHT, Proceedings of the International Conference on Semiconductors, Moscow, 1968 (Nauka, Leningrad, 1969) p. 1274.
4. A. YA. YAKUNIN and A. B. GLOT, *Izvestiya Vysshikh Vchebnykh Zavedenii Seriya Fizika* **5** (1975) 122.
5. R. R. VERDERBER and J. G. SIMMONS, *Radio Elec. Eng.* **23** (1967) 347.
6. "Scanning Electron Microscopy, 1970", Proceedings of the Third Annual Scanning Electron Microscope Symposium, April 1970 (ITT Research Institute, Chicago, USA) p. 417.
7. F. A. S. AL-RAMADHAN and C. A. HOGARTH, *J. Mater. Sci.* **19** (1984) 1718.
8. F. A. S. AL-RAMADHAN, C. A. HOGARTH and K. I. ARSHAK, *Int. J. Electron.* **57** (1984) 227.
9. D. V. MORGAN and M. J. HOWES, *Phys. Status Solidi (a)* **21** (1974) 191.
10. S. A. Y. AL-ISMAIL and C. A. HOGARTH, *J. Mater. Sci.* **18** (1983) 2777.
11. K. I. ARSHAK, F. A. S. AL-RAMADHAN and C. A. HOGARTH, *ibid.* **19** (1984) 1505.
12. A. E. HILL, A. M. PRAHLE and J. H. CALDERWOOD, *Thin Solid Films* **5** (1970) 287.
13. R. P. HOWSON and A. TAYLOR, *ibid.* **6** (1970) 31.

Received 18 October
and accepted 6 November 1984